Chemical Science

ROYAL SOCIETY OF CHEMISTRY

EDGE ARTICLE

View Article Online
View Journal | View Issue

Cite this: *Chem. Sci.*, 2025, **16**, 3336

All publication charges for this article have been paid for by the Royal Society of Chemistry

Received 23rd October 2024
Accepted 10th January 2025

DOI: 10.1039/d4sc07184k

rsc.li/chemical-science

Affinity-based covalent sialyltransferase probes enabled by ligand-directed chemistry†

Jun Yang Ong, [a] Erianna I. Alvarado-Melendez, [a] Joshua C. L. Maliepaard,[b] Karli R. Reiding [b] and Tom Wennekes *[a]

Sialyltransferases (ST) are key enzymes found in, among others, mammals and bacteria that are responsible for producing sialylated glycans, which play critical roles in human health and disease. However, chemical tools to study sialyltransferases have been limited to non-covalent inhibitors and probes that do not allow isolation and profiling of these important enzymes. Here we report a new class of covalent affinity-based probes (AfBP) for ST by using ligand-directed chemistry (LDchem). Our affinity-based probes are armed with a simple to synthesise but robust *O*-nitrobenzoxadiazole (*O*-NBD) warhead, which is a lysine-specific S_NAr electrophilic warhead with an advantageous turn-on fluorescence property. We chemoenzymatically synthesised a series of CMP-Neu5Ac based probes and demonstrated their high specificity in labelling a range of recombinant STs with submicromolar sensitivity. Importantly, with our LDchem ST probe, we successfully labelled the endogenous lipooligosaccharide ST (Lst) in live *Neisseria gonorrhoeae*, a clinically relevant human pathogen. Our results demonstrated that this new class of covalent ST probes offer a robust platform for ST profiling and future studies of STs in their native environments.

Introduction

Sialyltransferases (ST) are enzymes that catalyse sialylation, which is the transfer of sialic acids onto glycan chains. Sialylation plays many important roles in healthy human physiology, but has also been implicated as a key cancer and bacterial pathogenicity marker.[1–6] Various sialic acid mimics have been developed as reversible inhibitors and fluorescent probes to aid in the study of ST,[7–9] but their use is limited by the lack of a stable covalent linkage to the enzyme. While activity-based covalent probes (ABPs) have been successfully developed and proved invaluable in profiling and studying many glycosidases,[10–12] such probes have not been reported for ST or glycosyltransferases in general. This effort is in part hindered by the non-covalent, single displacement S_N2 catalytic mechanism by which all ST and many inverting glycosyltransferases operate[13–15] as supported by crystal structures and mechanistic studies.[16–25] In this mechanism, no covalent intermediate between the CMP-Neu5Ac substrate and the enzyme is formed (Scheme 1), therefore a stable covalent adduct cannot be trapped by stabilising such an intermediate, unlike what has been commonly done for the retaining glycosyl hydrolase ABPs.

On the other hand, an affinity-based probe (AfBP) overcomes this limitation because it does not depend on a covalent catalytic intermediate. A typical AfBP consists of three parts: (1) a ligand with high affinity to the target protein (the directing group); (2) a linker of appropriate length; (3) a reactive group (the warhead) that is capable of forming a covalent bond with an amino acid residue close by (Fig. 1A). One major type of AfBP is a photoaffinity probe, where the warhead is activated for chemical crosslinking upon photo-irradiation. A photoaffinity-based sialyltransferase probe was recently reported to selectively photocrosslink to purified recombinant human sialyltransferase ST6Gal1 over ST3Gal1 and ST3Gal4.[26] This probe, based on photoaffinity labeling (PAL), has the potential to become a valuable tool for studying STs, offering high spatio-temporal control and the ability to crosslink with various amino

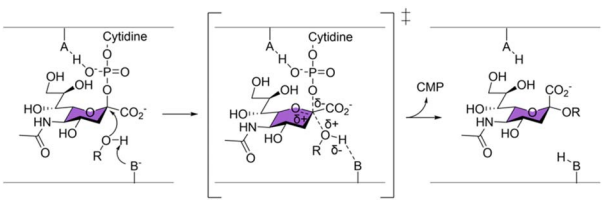

Scheme 1 All sialyltransferases characterised so far have been proposed to operate by a single displacement S_N2 mechanism.

[a]*Chemical Biology and Drug Discovery, Bijvoet Center for Biomolecular Research and Utrecht Institute for Pharmaceutical Sciences, Utrecht University, Universiteitsweg 99, 3584 CG Utrecht, The Netherlands. E-mail: t.wennekes@uu.nl*

[b]*Biomolecular Mass Spectrometry and Proteomics, Bijvoet Center for Biomolecular Research and Utrecht Institute for Pharmaceutical Sciences, Utrecht University, Netherlands Proteomics Center, 3584 CH Utrecht, The Netherlands*

† Electronic supplementary information (ESI) available. See DOI: https://doi.org/10.1039/d4sc07184k

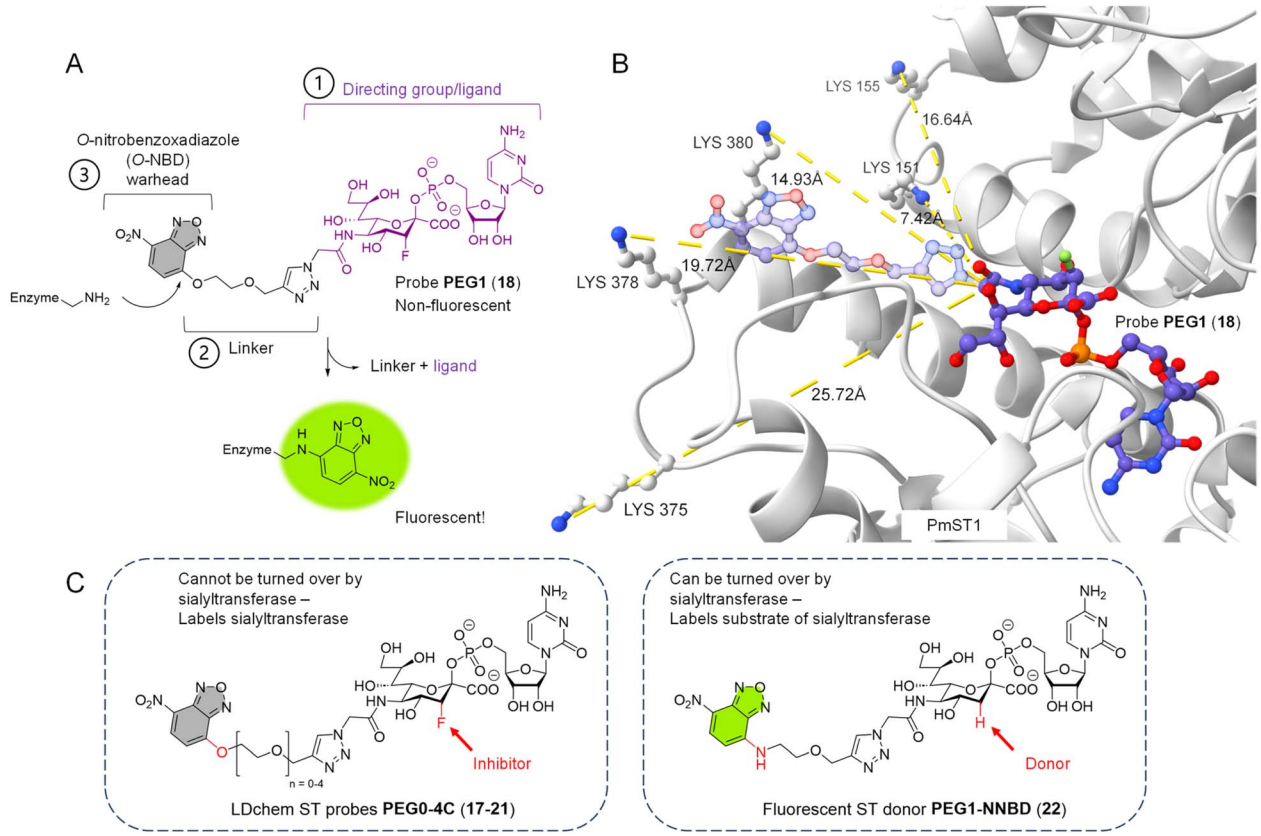

Fig. 1 Design of *O*-NBD armed sialyltransferase probes. (A) Turn-on fluorescence property of *O*-NBD warhead upon reacting with a lysine residue is highly advantageous to allow wash-free labelling and reduce background signals. Linker length of probe **PEG1** (**18**) is presented here. (B) Multiple lysines in the crystal structure of PmST1 WT (PDB: 2IHZ) are positioned close to the *N*-acetyl group of the bound CMP-3F(axial)-Neu5Ac ligand. The triazole-PEG1 linker and *O*-NBD group of probe **PEG1** (**18**) are modelled onto the ligand structure (represented in 50% transparency), showing the *O*-NBD warhead to be in close proximity to the lysine residues for possible directed reactivity. (C) Chemical structures of probes with different linker lengths **PEG0-4C** (**17–21**) and donor **22**. The differences (*O*/*N*-NBD, 3-F/H) between the two groups of reagents are highlighted in red. Linker lengths **PEG0-4C** in Å can be found in Table S2.†

acid residues. However, its high reactivity when activated often results in significant background interference.

In this paper, we report the facile chemical synthesis and biological validation of a new class of highly selective covalent AfBP for sialyltransferases using the principle of ligand-directed chemistry (LDchem). LDchem employs cleavable warheads whose activities are driven solely by proximity effect upon ligand binding, and which upon reaction, cleave and release the ligand to label the protein-of-interest with a reporter moiety in a traceless manner. The activation of an LDchem warhead only upon binding and long residence time of the ligand on the target protein also allows repeated equilibrium between the probe and the target protein over a longer period of time, thereby increases the signal-to-noise ratio (eqn (1), ESI†). This approach has been applied successfully in endogenous protein labelling and profiling.[27] However, its application in chemical glycobiology research is scarce, with only one example reported on isolated glycosidases.[28]

By screening for seven STs across four glycosyltransferase (GT) families, we show here that our LDchem ST probes are not only highly specific for a range of recombinant sialyltransferases, but also are capable of labelling the endogenous lipooligosaccharides (LOS) sialyltransferase Lst in live *Neisseria gonorrhoeae*, a clinically relevant human pathogen. We envision that our probes, with an efficient one-step labelling protocol, could serve as a valuable tool for endogenous ST profiling, complimentary to the photoaffinity technology.

Results and discussion

Rational design and synthesis of the covalent ST probes

Our design rationale for each part of the LDchem ST probes (Fig. 1A) is as follows:

(1) The ligand/directing group was selected based on the known universal sialyltransferase inhibitor CMP-3F(axial)-Neu5Ac (**7**), which is itself a non-hydrolysable mimic of CMP-Neu5Ac, the natural universal substrate of all sialyltransferases.

(2) Linkers were designed to span a distance from ~7 Å to ~23 Å (**PEG0-4C**) to systematically study the effect of the linker length on labelling efficiency. As we aimed to target non-catalytic lysines residues, these residues are not conserved and can lie at different distances from the active sites in different sialyltransferases. Furthermore, the linker is connected to the C5 position of the sialic acid in the ligand, as it has

been shown that the C5 *N*-acetyl group is solvent-exposed and can tolerate modifications without affecting binding to the sialyltransferases.

(3) *O*-Nitrobenzoxadiazole (*O*-NBD) is a lysine-specific S_NAr electrophilic warhead with a desirable turn-on fluorescence property.[29] The use of the *O*-NBD warhead in LDChem probes has been reported in several studies and has proven to be robust, notably for its stability in aqueous solution.[29–32]

The three parts of the probe were connected through a facile modular synthesis, namely (Part 2 + Part 3) + Part 1 (Schemes S1 and S2†) to give a panel of LDchem ST probes **PEG0-4C** (**17–21**). The crucial final step was facilitated by copper-catalysed azide–alkyne cycloaddition (CuAAC) between the chemoenzymatically synthesised azide-modified CMP-Neu5Ac-based ligand and the set of five alkyne-appended *O*-NBD warheads with varying linker length. Here, the remarkable aqueous stability of the *O*-NBD warhead, despite its high reactivity upon ligand binding, was fundamental to the successful assembly of the probe molecules, which due to their highly hydrophilic properties necessitate the use of water as the reaction solvent.

At the same time, we designed and synthesised a new fluorescently labelled CMP-sialic acid donor **PEG1-*N*-NBD** (**22**), which is isosteric to probe **PEG1** (**18**) but can act as a substrate to the sialyltransferases (Fig. 1C). This donor allows us to rapidly determine the activity of the sialyltransferases by tracking the fluorescently labelled products directly on a TLC plate or in a SDS-PAGE gel.

Details on the synthesis of the probes with varying linker length **PEG0-4C** (**17–21**) and donor **PEG1-*N*-NBD** (**22**) are provided in the ESI.†

Evaluation of the specificity and promiscuity of the ST probes

We selected seven ST with different linkage specificities (α2,3/2,6/2,8) from four different glycosyltransferase (GT) families and six different organism origins to investigate the specificity and the promiscuity of our affinity-based probes (Table 1). Both X-ray diffraction crystal structures and AlphaFold structure prediction of these enzymes showed at least one lysine residue in the vicinity of the sugar nucleotide binding site. The proximity of the *O*-NBD warhead to these lysine residues upon binding of the ligand was further verified by docking of our designed probes into the crystal structure of PmST1 (PDB: 2IHZ) (Fig. 1B).

All ST enzymes were expressed recombinantly, purified and tested for their activity prior to labelling experiments using donor **PEG1-*N*-NBD** (**22**) and lactose (Fig. S1†). This result also confirmed that the triazole-**PEG1-*N*-NBD** (and by structural homology, *O*-NBD) modification on the C5 position of the sialic acid was well tolerated and did not prevent the binding of the CMP-sialic acid derivatives to the sialyltransferases.

Standard labelling experiments were carried out in the presence of 1 μM sialyltransferase, 1 μM of sialic acid aldolase (as a background non-binding control protein to detect potential non-specific labelling) and 1 μM of probe **PEG0-4C** (**17–21**) in 25 mM pH 7.2 phosphate buffer at 37 °C for 2 hours. For all sialyltransferases, we observed a linker length-dependent labelling (Fig. 2 and S2†), with a detection limit down to 0.0625 μM of VJT-FAJ-16 and 0.125 μM of Cst-II (Fig. S3†). Labelling was observed even at pH 6.0, but when the pH of the reaction buffer was increased to 7.7 and 8.5, the labelling intensity increased as expected, without significant loss of selectivity (Fig. S4A and B†). We also observed exceptional stability of the probes when incubating them for 4 h in phosphate/Tris buffer in this pH range at 37 °C (Fig. S4C†). However, under all conditions, PmST1 M144D and ST6Gal1 showed minimal labelling (Fig. 2A and B).

Investigation of the contrasting labelling efficiency between PmST1 WT and its M144D mutant

To explain why a single amino acid difference led to the contrasting labelling efficiency between PmST1 WT and its M144D single mutant, we looked into their kinetics characterisation and crystal structures. Here it has been shown that there are marked differences in the protein conformation between the two variants and about a five times higher K_M for the donor for the M144D mutant (by comparison of the donor hydrolysis kinetics data).[18,33] There are therefore two possible factors that could cause the difference in labelling efficiency. Firstly, the homologous lysine residue which was labelled in PmST1 WT is positioned out of reach in PmST1 M144D mutant because of its altered conformation and therefore prevented the labelling. Secondly, the equilibrium dissociation constant (K_d) of the ligand is higher for the M144D mutant (lower affinity) than the WT enzyme, which would diminish the rate of the labelling reaction as predicted by eqn (1), ESI.†[39]

Table 1 List of sialyltransferases selected in this study

Sialyltransferase	Organism	GT family	Specificities	Crystal structure
PmST1 WT	*Pasteurella multocida*	GT80	2,3/2,6 ST	2IHZ (ref. 18)
PmST1 M144D	*Pasteurella multocida*	GT80	2,3 ST	3S44 (ref. 33)
VJT-FAJ-16 (ref. 34)	*Vibrio* sp. JT-FAJ-16	GT80	2,3 ST	A8R0Y0[a]
Pd2,6ST	*Photobacterium damselae*	GT80	2,6 ST	4R84 (ref. 35)
ST6Gal1	*Homo sapiens*	GT29	2,6 ST	4JS1 (ref. 36)
Cst-II	*Campylobacter jejuni*	GT42	2,3/2,8 ST	1RO7 (ref. 16)
N. gono Lst	*Neisseria gonorrhoeae*	GT52	2,3 ST	2YK7 (ref. 22)[b]

[a] AlphaFold structure prediction.[37,38] [b] NST from *N. meningitidis* L1 was used as homology for *N. gono* Lst.

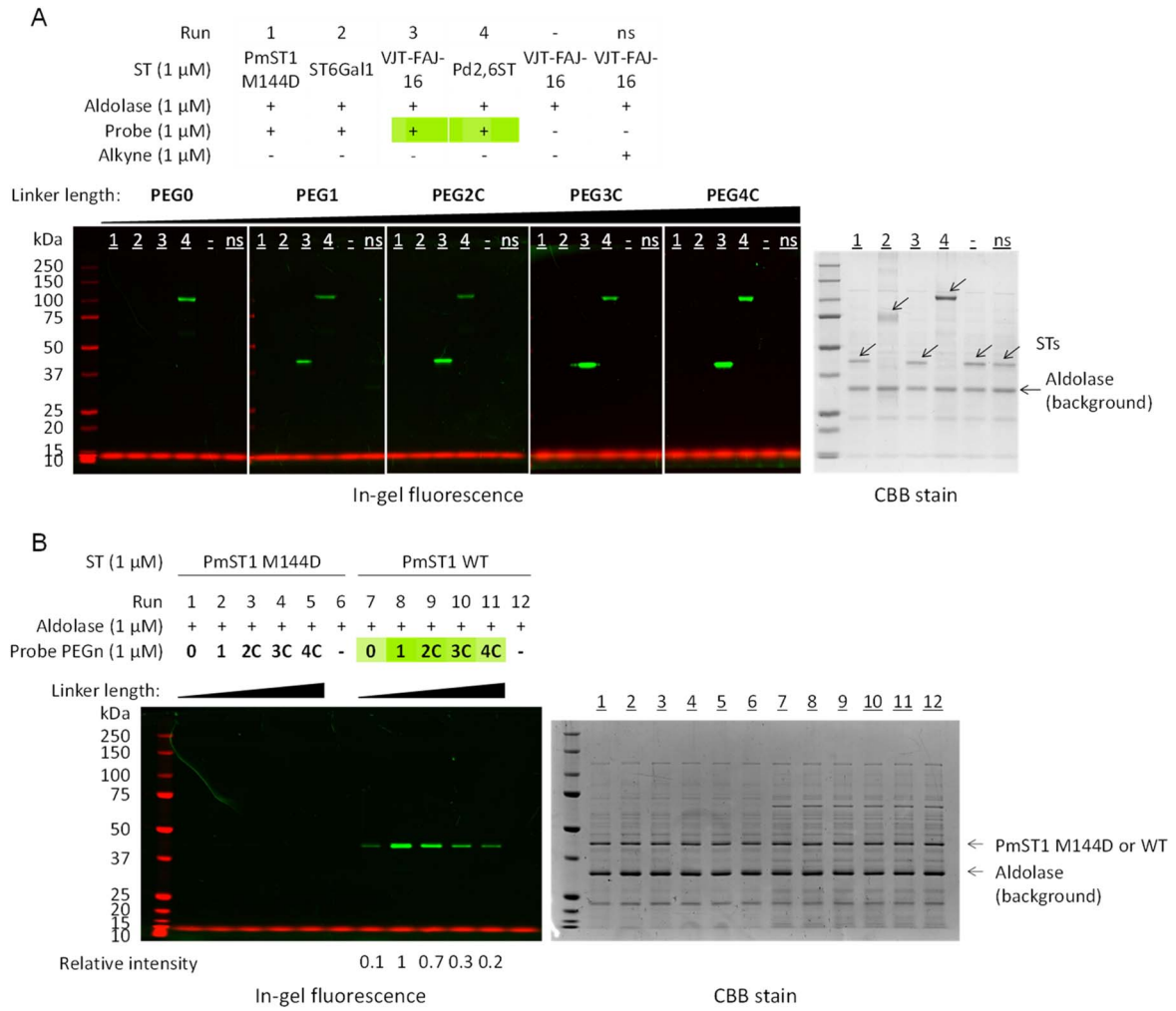

Fig. 2 In-gel fluorescence was used to analyse the effect of linker length on the labelling efficiency of PmST1 WT, PmST1 M144D, ST6Gal1, VJT-FAJ-16 and Pd2,6ST by the affinity-based probes **PEG0-4C** (**17–21**). (A) VJT-FAJ-16 and Pd2,6ST were labelled to different degrees by probes with linker length ranging from PEG0 to PEG4C, while PmST1 M144D and ST6Gal1 showed no labelling. (B) Side-by-side comparison of PmST1 WT and M144D single mutant showed contrasting labelling efficiency, although both enzymes were active and able to transfer donor **22** onto lactose efficiently (Fig. S1†). ns: non-specific labelling control, alkynes with the corresponding linker length (**8–9**, **13–15**) were used. In all experiments no off-target labelling was observed on the non-binding aldolase control (the aldolase is responsible for contributing the numerous background bands in the CBB). Relative intensity was measured by ImageJ.

To test the first hypothesis, we carried out bottom-up liquid chromatography-tandem mass spectrometry (LC-MS/MS) to identify the labelling site in PmST1 WT by probe **PEG1** (**18**) (Fig. S5, Table S3†). Rather surprisingly, proteomics revealed lysines K375 and K378 on the β12–α12a loop of PmST1 WT as the modification sites (SHIIFTSNKQVKSKED). These lysines were not expected from initial docking experiments because the β12–α12a loop (residues 374–382) was missing from all the ligand-bound crystal structures solved by two independent research groups due to its highly disordered nature (PDB: 2IHZ and 2IY8),[18,40] except for in the ligand-free apo structure (PDB: 2EX0).[41] However, we were able to reconstruct this region by using the One-to-One Threading function of Phyre2 with PDB: 2IHZ as the model (Fig. 1B).[42] On the other hand, sequence coverage on the N-terminal catalytic domain containing lysines K151 and K155 (DDGSMEYVDLEKEENKDIS) was limited, so they cannot be definitively excluded as potential labelling sites.

Dramatic conformational change upon binding to cytidine monophosphate (CMP) and CMP-3F(axial)-Neu5Ac (**7**) has been observed in PmST1 WT but not in its M144D mutant.[18,33] These changes include closing of the N-terminal domain and movement of the β12–α12a loop together with the β8–α8 loop, which contains the important gatekeeper tryptophan residue W270. This movement may be essential to bring the lysines K375 and K378 into the reacting distance of the *O*-NBD warhead, as illustrated by Movie 1 (see ESI†). Serendipitously, our labelling experiment thus provided further evidence for this lack of conformational change in PmST1 M144D upon donor binding, corroborating the earlier crystal structure and NMR studies,[33] and also shedding light on this disordered region that was unable to be observed by crystallography. However, we cannot dismiss the possibility that a higher K_d for the probes is also an equally important contributing factor for the lack of labelling in PmST1 M144D.

LC-MS/MS reveals anomalous labelling sites in VJT-FAJ-16

At the same time, LC-MS/MS was able to identify lysines K301 (FKGHPSATF) and K353 (SIPKEVKNKF) as the labelling sites in VJT-FAJ-16 (Fig. S5, Table S3†). This finding was highly interesting because K301 is located inside the binding pocket of CMP, and therefore its selectivity was not intuitive. We were confident that the modified CMP-sialic acids bind correctly in the catalytic pocket of VJT-FAJ-16 because the donor **PEG1-*N*-NBD** (**22**) could be successfully turned over by VJT-FAJ-16 (Fig. S1†). Subsequently, we carried out molecular docking of probe **PEG1** (**18**) and found a second *in silico* binding mode (Fig. S6D†), where the NBD could bind in the place of cytidine. Our hypothesis is that the probe first binds in the correct conformation with the CMP-sialic acid ligand in the catalytic binding site (Fig. S6A–C†), and statistical rebinding flips the molecule to position the *O*-NBD in the CMP binding pocket (Fig. S6D†). It is followed by the attack of K301 on the electrophilic centre of the *O*-NBD. Molecular docking also showed a third binding mode (Fig. S6E†) which justified the labelling of K353. This finding serves to remind us that although rational design of affinity-based probes is a powerful technique, one should always investigate their molecular-level activity by multiple techniques to identify unexpected modes of action.

Using turn-on fluorescence to measure the affinity of probe 18 for PmST1 WT and VJT-FAJ-16

We capitalised on the unique turn-on fluorescence property of the *O*-NBD probe to determine the binding affinity of probe **18** to the sialyltransferases. The fluorescence increase over time, as the labelled enzymes were formed, was measured and used to calculate the K_M of the labelling reaction using an adapted version of previously published eqn (1), ESI.†[43] The K_M of probe **PEG1** (**18**) was estimated to be 0.5 ± 0.1 μM for VJT-FAJ-16 and 0.6 ± 0.2 μM for PmST1 WT (Fig. 3). Since the estimated K_M represents the upper limit value for the K_d of the probe, we concluded that the probe has a binding affinity for both enzymes in the submicromolar concentration.

At the same time, we discovered that by taking into account a competitive inhibitor in the kinetics equation, we could establish a competition assay to measure the K_i of a competitive inhibitor. To evaluate our newly derived equation (eqn (2), full derivation available in the ESI†), we carried out a competition assay using various concentrations of the competitive inhibitor CMP-3F(axial)-Neu5Ac (**7**) (Fig. 3). The K_i for CMP-3F(axial)-Neu5Ac (**7**) was calculated to be 3.6 ± 0.5 μM for VJT-FAJ-16, while the K_i calculated for PmST1 WT was 19.2 ± 6.9 μM, which is close to the reported literature value of 25.7 μM.[18] These preliminary results presented a possible use of our LDchem ST probes for high-throughput screening of ST inhibitors, as an alternative to activity assay or fluorescent polarisation (FP) assay.

Absence of labelling of STGal1

We attributed the absence of labelling of ST6Gal1 to a low binding affinity. The crystal structure of ST6Gal1 clearly shows

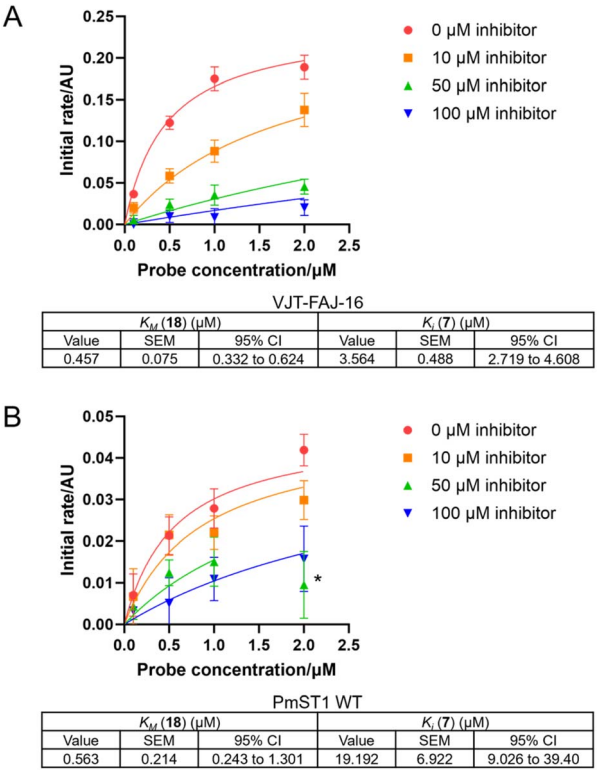

VJT-FAJ-16

K_M (**18**) (μM)			K_i (**7**) (μM)		
Value	SEM	95% CI	Value	SEM	95% CI
0.457	0.075	0.332 to 0.624	3.564	0.488	2.719 to 4.608

PmST1 WT

K_M (**18**) (μM)			K_i (**7**) (μM)		
Value	SEM	95% CI	Value	SEM	95% CI
0.563	0.214	0.243 to 1.301	19.192	6.922	9.026 to 39.40

Fig. 3 Kinetics curve fitting to eqn (2), ESI† was done to calculate K_M of the probe **PEG1** (**18**) and K_i of the competitive inhibitor CMP-3F(axial)-Neu5Ac (**7**) for (A) VJT-FAJ-16 and (B) PmST1 WT. *This outlier was omitted from curve fitting (2 μM probe, 50 μM inhibitor). n.b. Two independent experiments with duplicates were carried out for VJT-FAJ-16 with 0 μM and 100 μM inhibitor, and one experiment with duplicates was carried out for the rest. Error bars represent standard deviation (SD). Value of K_M and K_i were reported with their standard error of the mean (SEM) and 95% confidence interval (CI).

lysine residues in the vicinity of the ligand binding site, but CMP-3F(axial)-Neu5Ac (**7**) has been shown to bind only weakly to ST6Gal1 with a calculated dissociation constant (K_i) of 0.65 mM,[44] in contrast to 25.7 μM reported for PmST1 WT.[18] ST6Gal1 was also not able to transfer donor **PEG1-*N*-NBD** (**22**) efficiently (Fig. S1†), which was surprising given that ST6Gal1 has been shown to be tolerant of donor substrates modified at the C5 position of the sialic acid with either a biotin or a fluorophore.[45,46] All this suggested that the combination of modifications of the donor substrate analogues (probes **17–21**, donor **22**) led to a decrease in binding to ST6Gal1 and prevented efficient labelling or transfer.

Evaluation of probe specificity under crude conditions

To further prove the fidelity of the LDchem ST probes and their potential use in a more complex biological setting, we carried out a heat inactivation and competition assay by spiking 1 μM of VJT-FAJ-16 into 1 mg mL^{-1} of *E. coli* cell lysate (Fig. 4). This experiment confirmed the labelling as ligand-directed and demonstrated its high specificity in *E. coli* cell lysate.

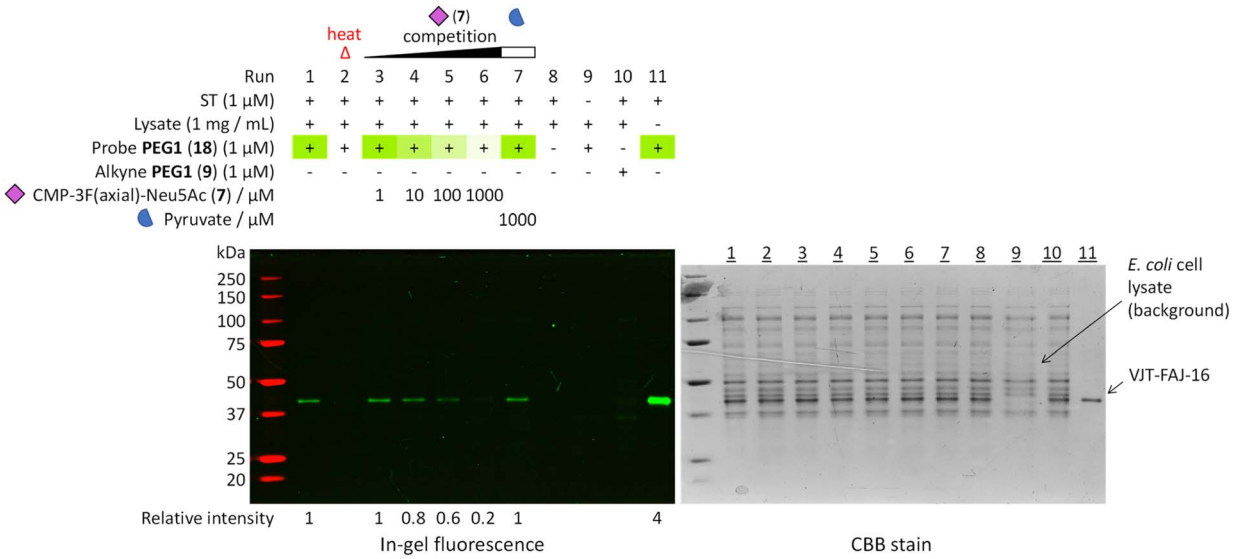

Fig. 4 Heat inactivation and a competition assay was used to further prove that the probes bind selectively to the active site of a properly folded sialyltransferase. Heat treatment denatured the enzyme and destroyed the binding pocket, resulting in no labelling. Increasing the concentration of active site competitor CMP-3F(axial)-Neu5Ac (**7**, ♦) decreased the labelling intensity while the same highest concentration of non-competitor pyruvate (❒) did not. All evidence pointed towards highly selective ligand-directed affinity-based labelling. Detailed procedure is described in the ESI.† Relative intensity was measured by ImageJ.

Labelling endogenous sialyltransferase Lst in live *N. gonorrhoeae* and its Triton X-100 extract

Finally, we investigated the possibility to label the endogenous Lst in *N. gonorrhoeae*, a relevant human pathogen that causes the sexually transmitted disease gonorrhoea. We attempted labelling under two conditions: in live *N. gonorrhoeae* and its Triton X-100 extract, as it has been demonstrated that it is an efficient method to extract sialyltransferase activity from *N. gonorrhoeae*.[47,48] Conveniently, a Lst-deficient mutant of *N. gonorrhoeae* F62 (strain JB1, referred to here as F62Δlst) was available[49,50] for direct comparison with the wild type F62.

Prior to affinity labelling, the presence of sialyltransferase activity in live bacteria and Triton X-100 extract was assessed using the native sialyltransferase (NST) bacteria labelling technique reported recently by our group.[46,51] With this technique, native LOS was used as the sialyltransferase acceptor and precluded the need to synthesise bespoke complex glycan acceptors. The Triton X-100 extract has also been shown previously to contain sufficient amount of LOS to allow us to detect the NST sialylation products.[47] Again we utilised the *N*-NBD fluorescently labelled CMP-sialic acid donor **PEG1-*N*-NBD** (**22**). With that, we were able to confirm sialyltransferase activity in *N. gonorrhoeae* F62 and the

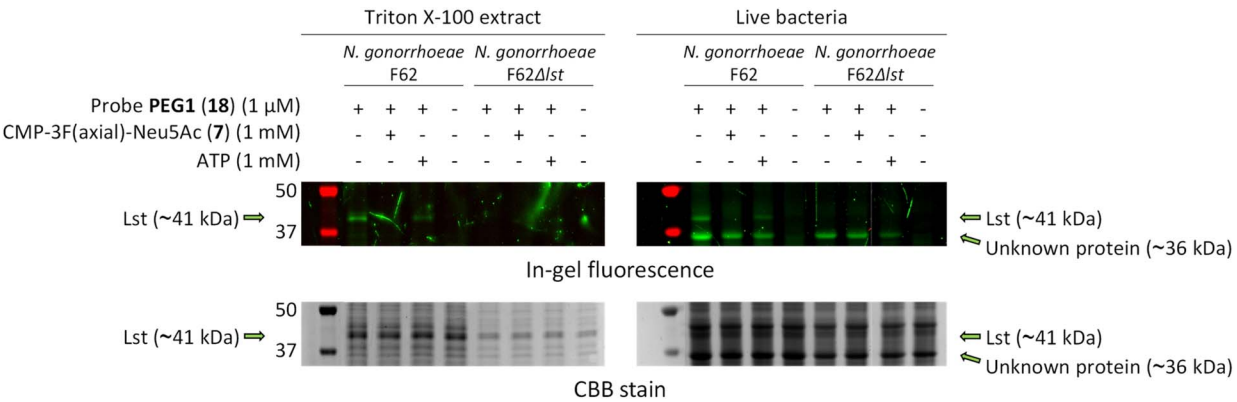

Fig. 5 Labelling of Lst was performed using probe **PEG1** (**18**) in live *N. gonorrhoeae* and its Triton X-100 extract. A labelled band at ~41 kDa that correspond to the molecular weight of Lst can be clearly seen in F62 and not F62Δlst, indicating successful labelling of the sialyltransferase in both live bacteria and Triton X-100 extract. Competition by CMP-3F(axial)-Neu5Ac completely abolished the labelling, providing additional evidence that the labelling was ligand-directed. An extra labelled protein (~36 kDa) was observed in live bacteria but not in the Triton X-100 extract, and it was postulated to be the neisserial porin PorB. Full uncropped gel images are presented in Fig. S8.†

absence thereof in F62Δlst by in-gel fluorescence and silver staining of the LOS, both in live bacteria and in the Triton X-100 extract (Fig. S7†).

Subsequently, we carried out affinity labelling in live *N. gonorrhoeae* and its Triton X-100 extract using 1 μM probe **PEG1** (**18**), which performed well with recombinant *N. gonorrhoeae* Lst. Similarly, we used competition with CMP-3F(axial)-Neu5Ac (**7**) to identify genuine ligand binding.

Excitingly, in both live bacteria and Triton X-100 extract, we could clearly see a labelled band at ~41 kDa that corresponds to the molecular weight of Lst only in F62 but not F62Δlst (Fig. 5), which also matched the observed band size on western blot in the study by Shell *et al.* using the same strain of *N. gonorrhoeae*.[52] The labelling could be competed off entirely by CMP-3F(axial)-Neu5Ac (**7**) and less efficiently by non-competitor ATP (although AMP can be present in the stock solution and is a weak competitive inhibitor for Lst).[47]

Interestingly, there was another labelled band at ~36 kDa that was observed only in live bacteria but not in the Triton X-100 extract. The fact that it was not extracted by 0.5% Triton X-100 suggested that it was likely integrally membrane bound. The identity of this protein is currently not known, but we speculate that it might be a major outer membrane protein (OMP), potentially the neisserial porin PorB that is known to bind nucleotides through lysine residues.[53,54] This could hint at its involvement in CMP-sialic acid uptake in *N. gonorrhoeae*, although prior studies have shown Lst to be a surface-exposed outer membrane protein.[52,55,56] Further study on this additional labelled protein is needed to determine if *N. gonorrhoeae* has another receptor protein for CMP-sialic acid.

Conclusions

In conclusion, we report here the utility of LDchem to develop highly specific covalent affinity-based probes for sialyltransferases. These *O*-NBD probes are straightforward to make, stable in water[57] and easy to analyse by turn-on fluorescence. Since these affinity-based probes do not target conserved catalytic residues, they are not expected to be universal. Their effectiveness depends on the presence of lysine residues near the binding site and a certain affinity threshold of the protein for the ligand. However, we show that the probes that we designed by this principle are promiscuous for many sialyltransferases in this study and are highly specific even in a complex biological setting such as in live bacteria. This modular ligand-directed approach, combined with alternative warheads, has the potential to expand the toolbox of covalent probes for previously inaccessible glycosyltransferases, which we have started investigating.

Data availability

Data associated with the LC-MS/MS experiments for this article are available at MassIVE repository at **https://doi.org/10.25345/C5VH5CW11** and can additionally be accessed *via* **https://MSV000095915@massive.ucsd.edu**. Other data supporting this article have been included as part of the ESI.†

Author contributions

J. Y. O. and T. W. conceived the research and designed the research approach. T. W. acquired the funding for this project. J. Y. O., E. I. A. and J. M. performed the experiments, collected and analyzed the raw data. T. W. and K. R. provided supervision. J. Y. O. wrote the initial manuscript with input from T. W. All authors contributed to the writing of the final version of the manuscript.

Conflicts of interest

There are no conflicts to declare.

Acknowledgements

We thank Prof. Dr Geert-Jan Boons (Utrecht University), Dr Gerlof P. Bosman (Utrecht University), Debóra van Ekeris (Utrecht University) and Dr Romane Breysse (Inbiose NV, Belgium) for kindly providing and assisting in the preparation of the recombinant enzymes. We thank Dr Javier Sastre Toraño for recording the high-resolution mass spectrometry data of synthesised chemical compounds. Research in this publication was supported by funding from the European Union's Horizon 2020 Marie Skłodowska-Curie Actions for the Innovative Training Network "Sweet Crosstalk" under the grant agreement No. 814102.

Notes and references

1 A. Varki, *Trends Mol. Med.*, 2008, **14**, 351–360.
2 X. Chen and A. Varki, *ACS Chem. Biol.*, 2010, **5**, 163–176.
3 E. R. Vimr, K. A. Kalivoda, E. L. Deszo and S. M. Steenbergen, *Microbiol. Mol. Biol. Rev.*, 2004, **68**, 132–153.
4 W. H. D. Bowles and T. M. Gloster, *Front. Mol. Biosci.*, 2021, **8**, 705133.
5 H. De Jong, M. M. S. M. Wösten and T. Wennekes, *Glycobiology*, 2022, **32**, 11–22.
6 A. J. Walklett, E. K. P. Flack, H. S. Chidwick, N. E. Hatton, T. Keenan, D. Budhadev, J. Walton, G. H. Thomas and M. A. Fascione, *Angew. Chem., Int. Ed.*, 2024, **63**, e202318523.
7 B. Müller, C. Schaub and R. R. Schmidt, *Angew Chem. Int. Ed. Engl.*, 1998, **37**, 2893–2897.
8 J. J. Preidl, V. S. Gnanapragassam, M. Lisurek, J. Saupe, R. Horstkorte and J. Rademann, *Angew. Chem., Int. Ed.*, 2014, **53**, 5700–5705.
9 K. Suzuki, A. Ohtake, Y. Ito and O. Kanie, *Chem. Commun.*, 2012, **48**, 9744.
10 M. D. Witte, G. A. Van Der Marel, J. M. F. G. Aerts and H. S. Overkleeft, *Org. Biomol. Chem.*, 2011, **9**, 5908–5926.
11 L. Wu, Z. Armstrong, S. P. Schröder, C. de Boer, M. Artola, J. M. Aerts, H. S. Overkleeft and G. J. Davies, *Curr. Opin. Chem. Biol.*, 2019, **53**, 25–36.
12 Y. M. C. A. Luijkx, S. Jongkees, K. Strijbis and T. Wennekes, *Org. Biomol. Chem.*, 2021, **19**, 2968–2977.
13 M. Audry, C. Jeanneau, A. Imberty, A. Harduin-Lepers, P. Delannoy and C. Breton, *Glycobiology*, 2011, **21**, 716–726.

14 Y. Li and X. Chen, *Appl. Microbiol. Biotechnol.*, 2012, **94**, 887–905.
15 L. L. Lairson, B. Henrissat, G. J. Davies and S. G. Withers, *Annu. Rev. Biochem.*, 2008, **77**, 521–555.
16 C. P. C. Chiu, A. G. Watts, L. L. Lairson, M. Gilbert, D. Lim, W. W. Wakarchuk, S. G. Withers and N. C. J. Strynadka, *Nat. Struct. Mol. Biol.*, 2004, **11**, 163–170.
17 C. P. C. Chiu, L. L. Lairson, M. Gilbert, W. W. Wakarchuk, S. G. Withers and N. C. J. Strynadka, *Biochemistry*, 2007, **46**, 7196–7204.
18 L. Ni, H. A. Chokhawala, H. Cao, R. Henning, L. Ng, S. Huang, H. Yu, X. Chen and A. J. Fisher, *Biochemistry*, 2007, **46**, 6288–6298.
19 Y. Kakuta, N. Okino, H. Kajiwara, M. Ichikawa, Y. Takakura, M. Ito and T. Yamamoto, *Glycobiology*, 2008, **18**, 66–73.
20 F. V. Rao, J. R. Rich, B. Raki, S. Buddai, M. F. Schwartz, K. Johnson, C. Bowe, W. W. Wakarchuk, S. Defrees, S. G. Withers and N. C. J. Strynadka, *Nat. Struct. Mol. Biol.*, 2009, **16**, 1186–1188.
21 H. J. Lee, L. L. Lairson, J. R. Rich, E. Lameignere, W. W. Wakarchuk, S. G. Withers and N. C. J. Strynadka, *J. Biol. Chem.*, 2011, **286**, 35922–35932.
22 L. Y. C. Lin, B. Rakic, C. P. C. Chiu, E. Lameignere, W. W. Wakarchuk, S. G. Withers and N. C. J. Strynadka, *J. Biol. Chem.*, 2011, **286**, 37237–37248.
23 L. Meng, F. Forouhar, D. Thieker, Z. Gao, A. Ramiah, H. Moniz, Y. Xiang, J. Seetharaman, S. Milaninia, M. Su, R. Bridger, L. Veillon, P. Azadi, G. Kornhaber, L. Wells, G. T. Montelione, R. J. Woods, L. Tong and K. W. Moremen, *J. Biol. Chem.*, 2013, **288**, 34680–34698.
24 C. Lizak, L. J. Worrall, L. Baumann, M. M. Pfleiderer, G. Volkers, T. Sun, L. Sim, W. Wakarchuk, S. G. Withers and N. C. J. Strynadka, *Sci. Rep.*, 2017, **7**, 1–13.
25 D. Harrus, A. Harduin-Lepers and T. Glumoff, *J. Struct. Biol.*, 2020, **212**, 107628.
26 D. Kumawat, T. E. Gray, C. R. Garnier, D. T. Bui, Z. Li, Z. Jame-Chenarboo, J. Jerasi, W. O. Wong, J. S. Klassen, C. J. Capicciotti and M. S. Macauley, *J. Am. Chem. Soc.*, 2024, **146**, 28630–28634.
27 K. Shiraiwa, R. Cheng, H. Nonaka, T. Tamura and I. Hamachi, *Cell Chem. Biol.*, 2020, **27**, 970–985.
28 H. Prasch, A. Wolfsgruber, M. Thonhofer, A. Culum, C. Mandl, P. Weber, M. Zündel, S. A. Nasseri, A. Gonzalez Santana, G. Tegl, B. Nidetzky, K. Gruber, A. E. Stütz, S. G. Withers and T. M. Wrodnigg, *ChemBioChem*, 2023, **24**, e202300480.
29 T. Yamaguchi, M. Asanuma, S. Nakanishi, Y. Saito, M. Okazaki, K. Dodo and M. Sodeoka, *Chem. Sci.*, 2014, **5**, 1021–1029.
30 M. Chen, M. Asanuma, M. Takahashi, Y. Shichino, M. Mito, K. Fujiwara, H. Saito, S. N. Floor, N. T. Ingolia, M. Sodeoka, K. Dodo, T. Ito and S. Iwasaki, *Cell Chem. Biol.*, 2021, **28**, 475.e8–486.e8.
31 K. R. Barnes, J. Blois, A. Smith, H. Yuan, F. Reynolds, R. Weissleder, L. C. Cantley and L. Josephson, *Bioconjugate Chem.*, 2008, **19**, 130–137.
32 D. Xue, L. Ye, J. Zheng, Y. Wu, X. Zhang, Y. Xu, T. Li, R. C. Stevens, F. Xu, M. Zhuang, S. Zhao, F. Zhao and H. Tao, *Org. Biomol. Chem.*, 2019, **17**, 6136–6142.
33 G. Sugiarto, K. Lau, J. Qu, Y. Li, S. Lim, S. Mu, J. B. Ames, A. J. Fisher and X. Chen, *ACS Chem. Biol.*, 2012, **7**, 1232–1240.
34 Y. Takakura, H. Tsukamoto and T. Yamamoto, *J. Biochem.*, 2007, **142**, 403–412.
35 N. Huynh, Y. Li, H. Yu, S. Huang, K. Lau, X. Chen and A. J. Fisher, *FEBS Lett.*, 2014, **588**, 4720–4729.
36 B. Kuhn, J. Benz, M. Greif, A. M. Engel, H. Sobek and M. G. Rudolph, *Acta Crystallogr., Sect. D: Biol. Crystallogr.*, 2013, **69**, 1826–1838.
37 J. Jumper, R. Evans, A. Pritzel, T. Green, M. Figurnov, O. Ronneberger, K. Tunyasuvunakool, R. Bates, A. Žídek, A. Potapenko, A. Bridgland, C. Meyer, S. A. A. Kohl, A. J. Ballard, A. Cowie, B. Romera-Paredes, S. Nikolov, R. Jain, J. Adler, T. Back, S. Petersen, D. Reiman, E. Clancy, M. Zielinski, M. Steinegger, M. Pacholska, T. Berghammer, S. Bodenstein, D. Silver, O. Vinyals, A. W. Senior, K. Kavukcuoglu, P. Kohli and D. Hassabis, *Nature*, 2021, **596**, 583–589.
38 M. Varadi, S. Anyango, M. Deshpande, S. Nair, C. Natassia, G. Yordanova, D. Yuan, O. Stroe, G. Wood, A. Laydon, A. Zídek, T. Green, K. Tunyasuvunakool, S. Petersen, J. Jumper, E. Clancy, R. Green, A. Vora, M. Lutfi, M. Figurnov, A. Cowie, N. Hobbs, P. Kohli, G. Kleywegt, E. Birney, D. Hassabis and S. Velankar, *Nucleic Acids Res.*, 2022, **50**, D439–D444.
39 D. E. Fahrney and A. M. Gold, *J. Am. Chem. Soc.*, 1963, **85**, 997–1000.
40 D.-U. Kim, J.-H. Yoo, Y.-J. Lee, K.-S. Kim and H.-S. Cho, *BMB Rep.*, 2008, **41**, 48–54.
41 L. Ni, M. Sun, H. Yu, H. Chokhawala, X. Chen and A. J. Fisher, *Biochemistry*, 2006, **45**, 2139–2148.
42 L. A. Kelley, S. Mezulis, C. M. Yates, M. N. Wass and M. J. E. Sternberg, *Nat. Protoc.*, 2015, **106**(10), 845–858.
43 D. E. Fahrney and A. M. Gold, *J. Am. Chem. Soc.*, 1963, **85**, 997–1000.
44 S. Liu, NMR active substrates for structure and function studies of sialyltransferases, PhD Thesis, University of Georgia, Athens, US, 2008.
45 T. Sun, S.-H. Yu, P. Zhao, L. Meng, K. W. Moremen, L. Wells, R. Steet and G.-J. Boons, *J. Am. Chem. Soc.*, 2016, **138**, 11575–11582.
46 H. de Jong, M. J. Moure, J. E. M. Hartman, G. P. Bosman, J. Y. Ong, B. W. Bardoel, G. J. Boons, M. M. S. M. Wösten and T. Wennekes, *ChemBioChem*, 2022, **23**, e202200340.
47 R. E. Mandrell, H. Smith, G. A. Jarvis, J. McLeod Griffiss and J. A. Cole, *Microb. Pathog.*, 1993, **14**, 307–313.
48 M. Packiam, D. M. Shell, S. V. Liu, Y.-B. Liu, D. J. McGee, R. Srivastava, S. Seal and R. F. Rest, *Infect. Immun.*, 2006, **74**, 2637–2650.
49 J. Bramley, R. D. de Hormaeche, C. Constantinidou, X. Nassif, N. Parsons, P. Jones, H. Smith and J. Cole, *Microb. Pathog.*, 1995, **18**, 187–195.

50 M. J. Gill, D. P. Mcquillen, J. P. M. Van Putten, L. M. Wetzler, J. Bramley, H. Crooke, N. J. Parsons, J. A. Cole and H. Smith, *Infect. Immun.*, 1996, **64**, 3374–3378.
51 E. I. Alvarado-Melendez, H. Jong, J. E. M. Hartman, J. Y. Ong, M. M. S. M. Wösten and T. Wennekes, *Glycobiology*, 2024, **34**, cwae071.
52 D. M. Shell, L. Chiles, R. C. Judd, S. Seal and R. F. Rest, *Infect. Immun.*, 2002, **70**, 3744–3751.
53 T. Rudel, A. Schmid, R. Benz, H. A. Kolb, F. Lang and T. F. Meyer, *Cell*, 1996, **85**, 391–402.
54 M. Tanabe, C. M. Nimigean and T. M. Iverson, *Proc. Natl. Acad. Sci. U. S. A.*, 2010, **107**, 6811–6816.
55 L. Gao, L. Linden, N. J. Parsons, J. A. Cole and H. Smith, *Microb. Pathog.*, 2000, **28**, 257–266.
56 F. E. C. Jen, M. R. Ketterer, E. A. Semchenko, C. J. Day, K. L. Seib, M. A. Apicella and M. P. Jennings, *mBio*, 2021, **12**, 1–11.
57 M. Kosar, D. A. Sykes, A. E. G. Viray, R. M. Vitale, R. C. Sarott, R. L. Ganzoni, D. Onion, J. M. Tobias, P. Leippe, C. Ullmer, E. A. Zirwes, W. Guba, U. Grether, J. A. Frank, D. B. Veprintsev and E. M. Carreira, *J. Am. Chem. Soc.*, 2023, **145**, 15094–15108.